Electronic Supplementary Information for Softness Matters: Effects of Compression on the Behavior of Adsorbed Microgels at Interfaces

Yuri Gerelli,[*,†] Fabrizio Camerin,[*,‡] Steffen Bochenek,[¶] Maximilian M. Schmidt,[¶] Armando Maestro,[§,‖,⊥] Walter Richtering,[¶] Emanuela Zaccarelli,[†] and Andrea Scotti[*,#]

†Italian National Research Council - Institute for Complex Systems (CNR-ISC), Sapienza University of Rome, Piazzale Aldo Moro 5, 00185 Rome, Italy

‡Division of Physical Chemistry, Lund University, P.O. Box 124, SE-22100 Lund, Sweden

¶Institute of Physical Chemistry, RWTH Aachen University, Landoltweg 2, 52056 Aachen, Germany

§Centro de Física de Materiales (CSIC, UPV/EHU) - Materials Physics Center MPC, Paseo Manuel de Lardizabal 5, E-20018 San Sebastián, Spain.

‖IKERBASQUE-Basque Foundation for Science, Plaza Euskadi 5, Bilbao, 48009 Spain.

⊥Institut Laue-Langevin, 71 Avenue des Martyrs, 38042 Grenoble, France

#Department of Biomedical Science, Faculty of Health and Society, Malmö University, SE-205 06 Malmö, Sweden

E-mail: yuri.gerelli@cnr.it; fabrizio.camerin@gmail.com; andrea.scotti@fkem1.lu.se

Compression isotherms

The mechanical properties of monolayers of soft and hard microgels were probed at the air-water interface. Compression isotherms were measured using a KSV-NIMA Langmuir trough (Biolin Scientific Oy) equipped with two parallel-moving barriers. The trough and the barriers were made of polyoxymethylene. Compression of microgel monolayers was achieved by closing the barriers at a speed of 10 mm/min. The surface pressure was measured by the Wilhelmy plate method utilizing a roughened platinum plate. The plate was placed perpendicular to the long axis of the trough and connected to a pressure sensor acquiring data in a continuous mode. For temperature control, the troughs were connected to an external water bath and circulating thermostated water through the base of the troughs. Ultrapure water (Astacus^2, membraPure GmbH, Germany), with a resistivity of 18.2 MOhm·cm was used as aqueous sub-phase. Aqueous solutions of microgels (concentration of 10 mg mL^{-1}) were mixed with 50 vol% of propan-2-ol (Merck KGaA, Germany) to facilitate spreading. For each measurement, the Langmuir trough was cleaned and a fresh air-water interface was created. After filling the water, the aqueous subphase was subjected to temperature equilibration and the surface was cleaned by suction. Then the solution was spread at the interface by dropwise addition with a μL syringe. After addition of the microgels, the interface was let to set for 30 minutes before compression began. Compression isotherms were all conducted at (20.0 ± 0.5) °C and are shown in Fig. S1 for the hard (squares) and soft microgels (circles).

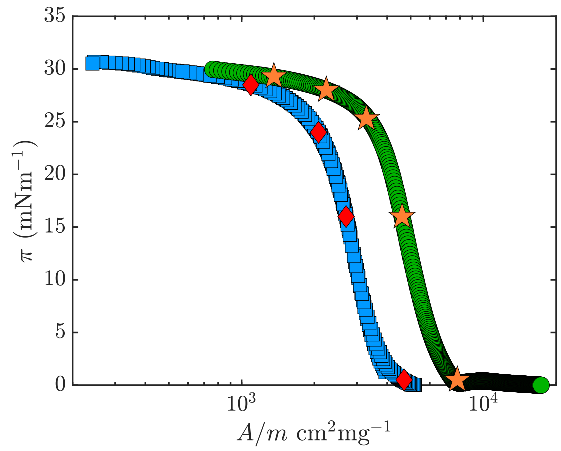

Figure S1: Compression isotherms for the hard (blue squares) and soft (green circles) microgels measured at the air-water interface at $T = 20 \pm 0.5$ °C. Diamonds and stars represents the points corresponding to the computer simulations performed for hard and soft microgels, respectively

NR modeling

The analysis of the NR data was based on the optimisation of a volume fraction profile (VFP) describing the microgel at the air-ACMW interface. The VFP of the microgel was modeled as the sum of a rising error function, $r(z)$, a decaying one, $d(z)$ and of a Gaussian peak, $g(z)$. $r(z)$ and $d(z)$ were used to describe the protrusion of the microgel in the air and in the water phases respectively. They were assumed to have equal amplitude to have a constant baseline value for the peak region.

$$g(z) = A_g e^{-\frac{1}{2}\left(\frac{z-Z_0}{w_g}\right)^2} \tag{S1}$$

$$r(z) = \frac{A_r}{2} erf\left(\frac{z - Z_r - Z_0}{\alpha_r(Z_0 - Z_r)}\right) \tag{S2}$$

$$d(z) = -\frac{A_r}{2} erf\left(\frac{z - Z_d + Z_0}{\alpha_d(Z_d - Z_0)}\right) \tag{S3}$$

The microgel VFP is therefore $\phi_{\mu g}(z) = r(z) + d(z) + g(z)$. The parameters used in Equations S1, S2, and S3 are:

- A_r: amplitude of the error function profiles;

- A_g: amplitude of the peak function;
- Z_0, Z_r and Z_d: position along the z-axis (orthogonal to the interface) of the Gaussian peak, and of the rising and decaying error functions, respectively;
- α_d and α_r: stretching parameters associated to the steepness of the error functions, α=0: step function, $\frac{1}{3} < \alpha < \frac{1}{2}$: fully stretched profile;
- w_g: Gaussian width;

The use of stretching parameters α to describe the steepness of the error functions is necessary to keep the shape of the profiles within meaningful physical limits. Indeed, if the error function is too stretched it does not reach, within a fixed $z-$range, the expected asymptotic values and, therefore, the generated profile will not match the nominal parameter values.

The full extension of the microgel VFP along z ($w_r + w_d$) can be determined from the position of the error functions inflection point as depicted in Figure S2, where $w_r = Z_0 - Z_r$ and $w_d = Z_d - Z_0$ indicate the extension of the protrusions above and below the interface.

The VFP of the gas and liquid phases were described by error functions with width fixed to $\sigma_{cw} = 0.3$ nm, to represent the surface roughness due to capillary waves for a free water surface at ambient pressure and temperature. Since by definition all VFP contributions must have sum 1 for every z-point, the air and water VFPs were defined as

$$\phi_{air}(z) = \frac{1}{2}\left[erf\left(\frac{z}{\sigma_{cw}}\right) + 1\right] \times [1 - \phi_{\mu g}(z)] \quad \text{(S4)}$$

$$\phi_w(z) = [1 - \phi_{air}(z)] \times [1 - \phi_{\mu g}(z)] \quad \text{(S5)}$$

Generic VFP profiles of microgel layer and air and water phases are given in Figure S2(a). In Figure S2(b) the individual contributions to the microgel VFP of $r(z) + d(z)$ and of $g(z)$ are shown together with the visual indication of the model parameters.

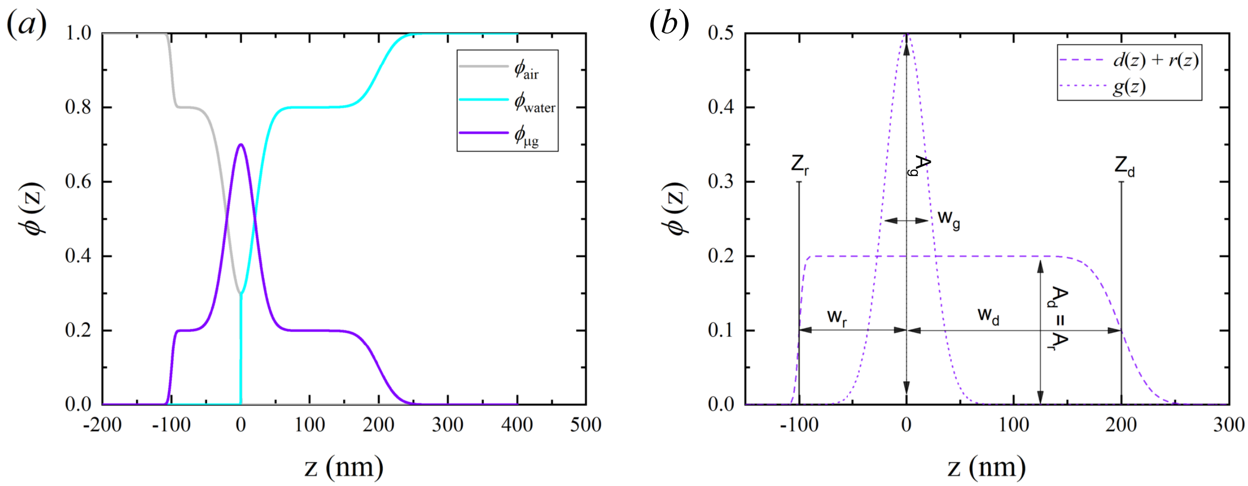

Figure S2: (a) Generic volume fraction profile for a microgel layer at the air-water interface. The partial contributions of air (ϕ_{air}, gray), water (ϕ_{water}, cyan) and polymer ($\phi_{\mu g}$, purple) are indicated. (b) Visual description of the microgel VFP model described by Equations S2, S3, and S1.

The computation of the theoretical reflectivity was performed as described in the main manuscript.

Microgel protrusion parameters

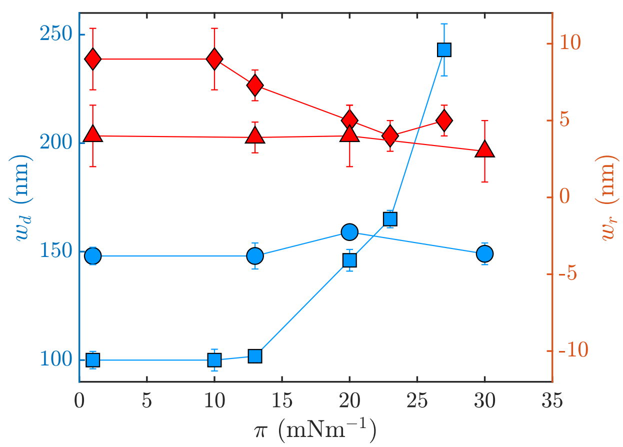

Figure S3: Extension of the protrusions in water (w_d, circles and squares, left axis) and in air (w_r, diamonds and triangles, right axis) for hard (squares and diamonds) and soft (circles and triangles) microgels as a function of the surface pressure π.

Confidence intervals for fits and $\phi(z)$

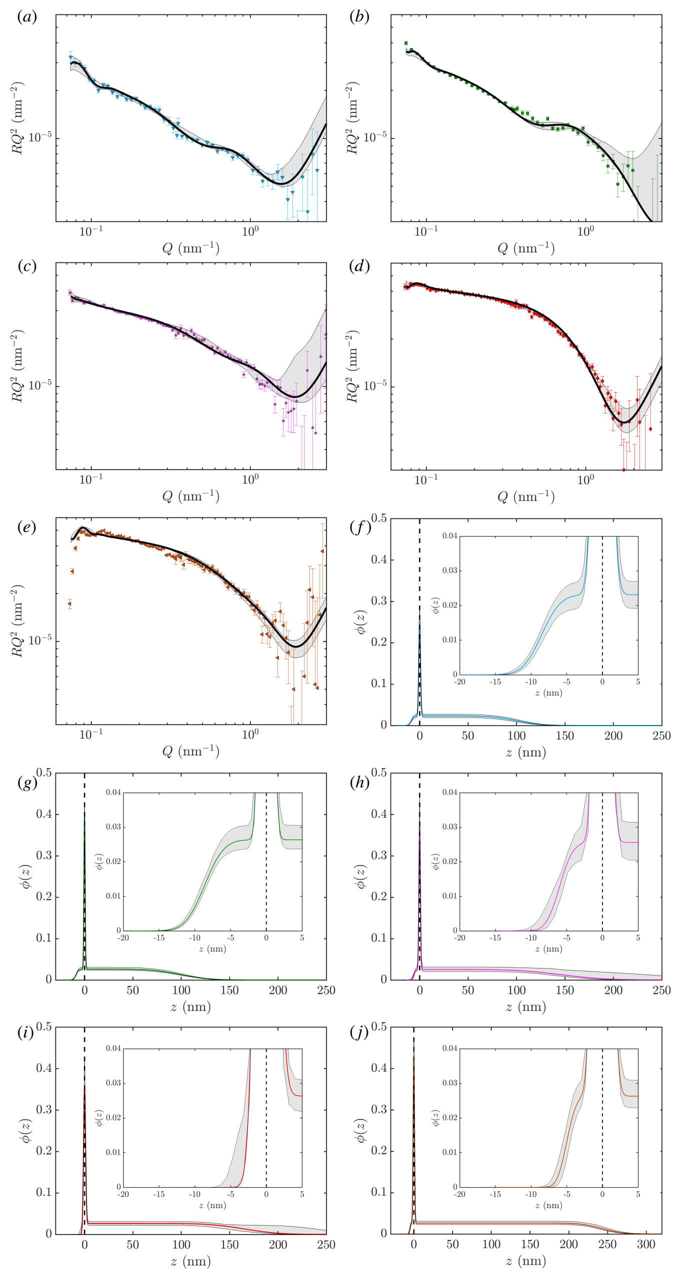

Figure S4: (a)-(e) Neutron reflectivity $R(Q)$ multiplied by Q^2 plotted as a function of the exchanged wave-vector Q (symbols) with the corresponding fits (solid line) and 95% (1.96 standard deviation) confidence intervals (shaded area). The symbols and surface pressure are the same used in Fig. 2. (f)-(j) Polymer volume fraction profiles (solid line) and corresponding confidence intervals (shaded area) as a function of the distance from the interface located at $z = 0$ nm (dashed vertical line), corresponding to the model NR curves displayed in panel (a)-(e).

Simulations

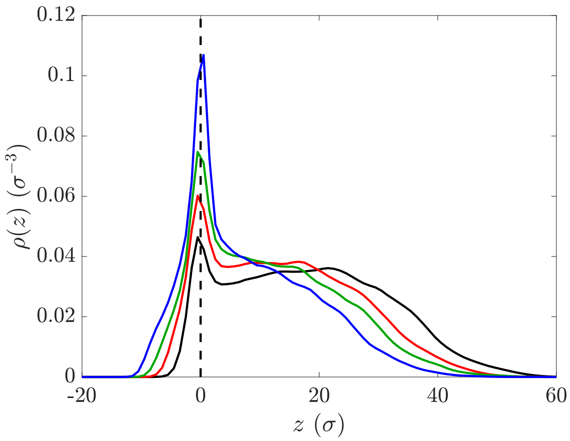

Figure S5: Microgel density profiles $\rho(z)$ computed from the simulation box containing a single hard microgel particle at different compressions, corresponding to experimental surface pressure values π= 1 (blue line), 16 (green line), 24 (red line) and 28 (black line) mNm^{-1}. Surface pressure values were obtained by correlating the generalized area fraction ζ_{2D} used in simulations with that employed in surface pressure experiments as described in the main manuscript. For clarity, the interface is located at z=0 and the air and water phases at $z < 0$ and $z > 0$ respectively.

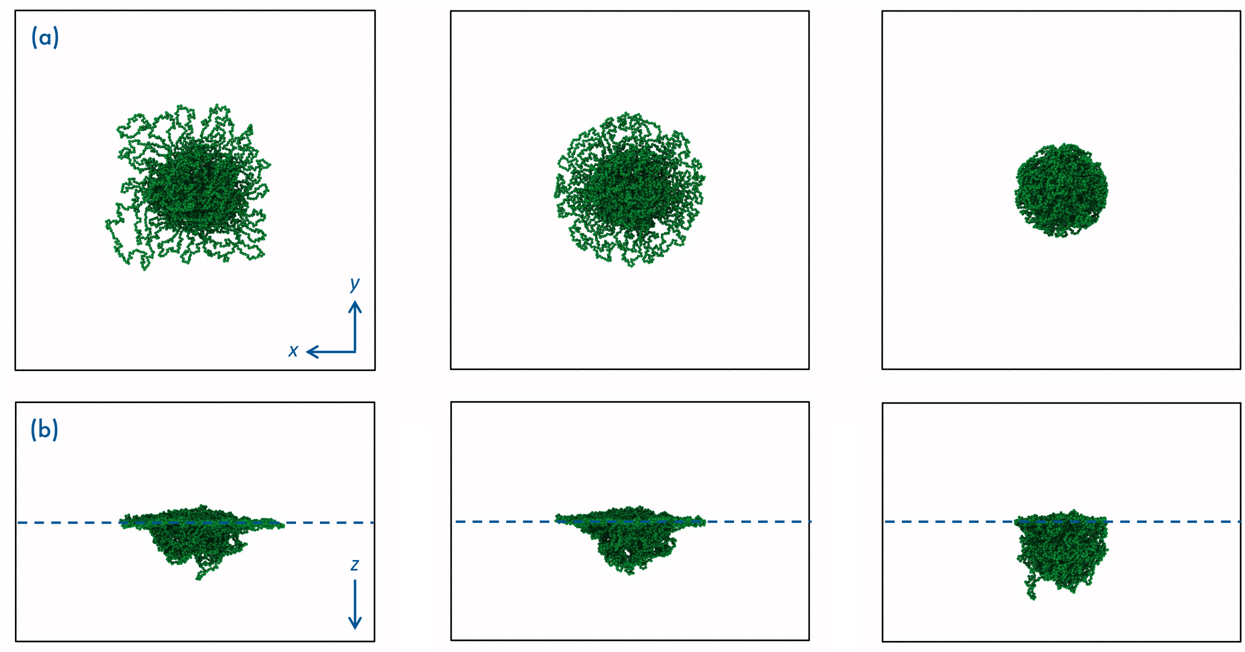

Figure S6: Representative simulation snapshots showing the compression of a single 5% crosslinked microgel by means of an external force of cylindrical symmetry with z as the main axis, from (a) top and (b) lateral views. Snapshots (from left to right) correspond to experimental surface pressure values π =1, 24, and 28 mN m^{-1}. These values were obtained by correlating the generalized area fraction ζ_{2D} used in simulations with that employed in surface pressure experiments as described in the main manuscript. The dashed line helps identifying the plane of the interface. Water is not shown for clarity.

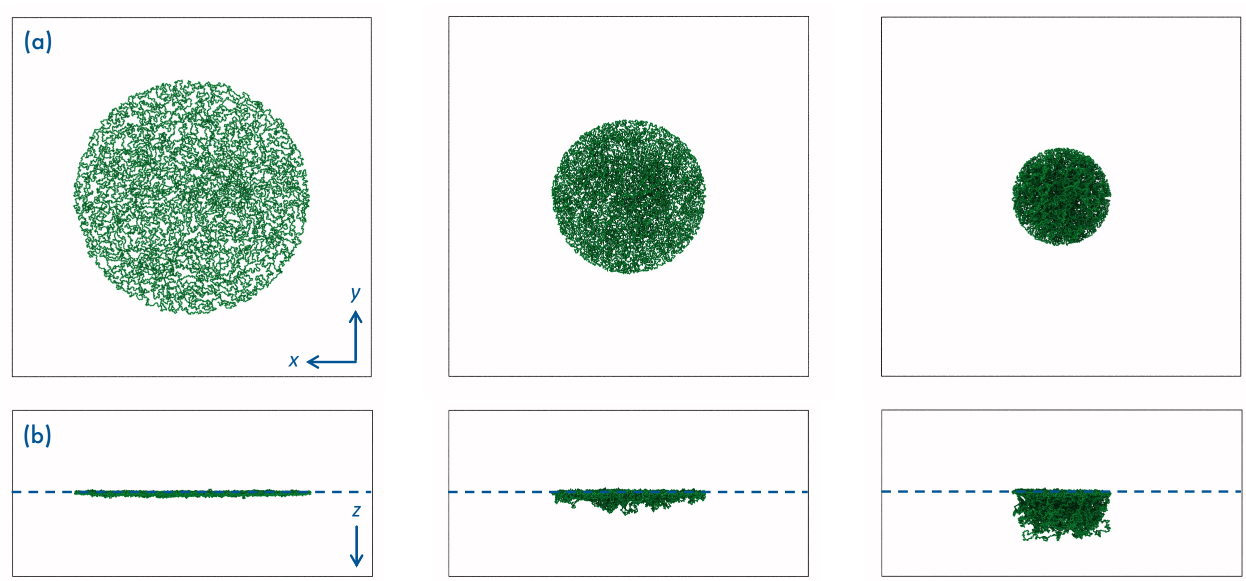

Figure S7: Representative simulation snapshots showing the compression of a single ULC microgel by means of an external force of cylindrical symmetry with z as the main axis, from (a) top and (b) lateral views. Snapshots (from left to right) correspond to experimental surface pressure values π =1, 25, and 29 mN m^{-1}, from left to right. These values were obtained by correlating the generalized area fraction ζ_{2D} used in simulations with that employed in surface pressure experiments as described in the main manuscript. The dashed line helps identifying the plane of the interface. Water is not shown for clarity.